

Selectivity in substitution chemistry of mixed-metal, tetrahedral MCo3 (M = iron, ruthenium) carbonyl clusters: cobalt-59 NMR study and crystal structure of RuCo3(.mu.3-H)(.mu.-CO)3(CO)8(NMe3)

Pierre Braunstein, Lionel Mourey, Jacky Rosé, Pierre Granger, Thierry Richert, Fadila Balegroune, Daniel Grandjean

▶ **To cite this version:**

Pierre Braunstein, Lionel Mourey, Jacky Rosé, Pierre Granger, Thierry Richert, et al.. Selectivity in substitution chemistry of mixed-metal, tetrahedral MCo3 (M = iron, ruthenium) carbonyl clusters: cobalt-59 NMR study and crystal structure of RuCo3(.mu.3-H)(.mu.-CO)3(CO)8(NMe3). Organometallics, 1992, 11 (7), pp.2628-2634. 10.1021/om00043a054 . hal-03004821

HAL Id: hal-03004821

https://cnrs.hal.science/hal-03004821

Submitted on 20 Nov 2020

HAL is a multi-disciplinary open access archive for the deposit and dissemination of scientific research documents, whether they are published or not. The documents may come from teaching and research institutions in France or abroad, or from public or private research centers.

L'archive ouverte pluridisciplinaire **HAL**, est destinée au dépôt et à la diffusion de documents scientifiques de niveau recherche, publiés ou non, émanant des établissements d'enseignement et de recherche français ou étrangers, des laboratoires publics ou privés.

Selectivity in Substitution Chemistry of Mixed-Metal, Tetrahedral MCo_3 (M = Fe, Ru) Carbonyl Clusters: ^{59}Co NMR Study and Crystal Structure of $RuCo_3(\mu_3\text{-}H)(\mu\text{-}CO)_3(CO)_8(NMe_3)$

Pierre Braunstein,* Lionel Mourey, and Jacky Rosé

Laboratoire de Chimie de Coordination, URA 416 CNRS, Université Louis Pasteur, 4 rue Blaise Pascal, 67070 Strasbourg Cédex, France

Pierre Granger and Thierry Richert

Unité Mixte 50 CNRS-Bruker-ULP, Université Louis Pasteur, BP 296/R8, 67008 Strasbourg Cédex, France

Fadila Balegroune and Daniel Grandjean

Laboratoire de Cristallochimie, URA 254, Université de Rennes I, Avenue du Général Leclerc, 35042 Rennes Cédex, France

Received January 30, 1992

Reactions between tetrahedral mixed-metal clusters $HMCo_3(CO)_{12}$ [M = Fe (**1a**), M = Ru (**1b**)] and trimethylamine *N*-oxide have led to the formation of the amine-substituted clusters $HMCo_3(CO)_{11}(NMe_3)$ [M = Fe (**2a**), M = Ru (**2b**)] in high yields. ^{59}Co NMR and IR spectroscopy were used to study the site selectivity of these reactions and indicate that substitution of the amine for the CO ligand takes place preferentially at one of the cobalt atoms. Clusters **2** are labile in solution and transform in the corresponding anions $[Me_3NH][MCo_3(CO)_{12}]$, owing to decoordination of the amine. Substitution reactions of the amine with other 2e donor ligands (PPh_3, SEt_2) were also studied. Disubstituted clusters were prepared under mild conditions and the very labile $HMCo_3(CO)_{10}(NMe_3)_2$, in which two cobalt atoms carry each an amine ligand, was characterized by ^{59}Co NMR spectroscopy. The structure of **2b** has been determined by X-ray diffraction: space group $Pna2_1$ with a = 16.877 (5) Å, b = 10.296 (2) Å, c = 11.946 (2) Å, $\alpha = \beta = \gamma = 90°$, and $Z = 4$. The structure was refined to $R = 0.026$ and $R_w = 0.035$ on the basis of 1471 reflections having $F_o^2 > 3\sigma(F_o^2)$. The cluster has a tetrahedral structure and the amine is axially bonded to a basal cobalt atom.

Introduction

Clusters provide excellent opportunities for studying the factors which lead to site-selective chemical reactions. Identification of the site of reagent attack requires unambiguous structural or spectroscopic information.[1] Transition metal carbonyl clusters with tetrahedral structures have been much investigated.[2] Phosphine ligands, for example, have been shown to substitute a carbonyl ligand bound to a basal cobalt atom in $Co_4(CO)_{12}$, occupying an axial site,[3] but equilibrium between axial and equatorial substitution was observed with $Rh_4(CO)_{11}(PPh_3)$.[4]

An additional question with mixed-metal clusters is that of their metalloselective transformation. Thus, in MCo_3 carbonyl clusters, ligand substitution could occur at M or cobalt. In all the structurally characterized tetrahedral $FeCo_3$ and $RuCo_3$ clusters, monosubstitution by phosphine is always observed at cobalt,[5-8] e.g., $HFeCo_3(CO)_{11}(PPh_2H)$[6], where the phosphine ligand is axially bound to a cobalt center. A similar situation has been found in $HRuCo_3(CO)_{11}(PR_2R')$.[7,8] Interestingly, equatorial substitution at a basal Rh was observed in the related $HRuRh_3(CO)_{11}(PR_3)$.[8] With other 2e donor ligands, the situation might be different, but $HRuCo_3(CO)_{11}(TeMe_2)$, where substitution has occurred on Ru, appears to be the only structurally characterized example of monosubstitution at an apical site in these series of clusters.[9] With phosphines, introduction of a second substituent could occur at another basal site or at the apical position. In homometallic clusters, the site occupied by the second and third incoming ligands depends upon the size of the ligand: small ligands, such as $P(OMe)_3$, enter axial sites and larger ligands progressively substitute on different basal metal atoms, as far away from the first ligand as possible.[10] Thus, in $Rh_4(CO)_{10}(PPh_3)_2$ and in $Ir_4(CO)_{10}(PPh_3)_2$, the phosphine ligands occupy an axial and an equatorial site,[4,11] while in $Co_4(CO)_{10}[P(OMe)_3]_2$, the two phosphite ligands are axially bonded to basal cobalt atoms.[3a] In contrast, a marked tendency to substitute in axial sites on basal metal atoms was observed for heterometallic clusters.[12] In $HRuCo_3(CO)_{10}(PPh_3)_2$, each phosphine is axially bound to a basal cobalt center,[13] but this should be contrasted with $HRuCo_3(CO)_{10}(PMe_2Ph)_2$, in which the second phosphine has substituted at the apical ruthenium.[14] Furthermore, in $HFeCo_3(CO)_9[P(OMe)_3]_3$, all three phosphite ligands occupy axial sites of the Co_3 base,[15]

(1) See, for example: Roland, E.; Vahrenkamp, H. *Organometallics* **1983**, *2*, 183. Shapley, J. R.; McAteer, C. H.; Churchill, M. R.; Biondi, L. V. *Organometallics* **1984**, *3*, 1595. Sappa, E.; Tiripicchio, A.; Braunstein, P. *Coord. Chem. Rev.* **1985**, *65*, 219. Horvath, I. T.; Zsolnai, L.; Huttner, G. *Organometallics* **1986**, *5*, 180. Johnston, P.; Hutchings, G. J.; Denner, L.; Boeyens, J. C. A.; Coville, N. J. *Organometallics* **1987**, *6*, 1292.

(2) Chini, P.; Heaton, B. T. *Top. Curr. Chem.* **1977**, *71*, 1.

(3) (a) Darensbourg, D. J.; Incorvia, M. J. *Inorg. Chem.* **1981**, *20*, 1911. (b) Bartl, K.; Boese, R.; Schmid, G. *J. Organomet. Chem.* **1981**, *206*, 331.

(4) Heaton, B. T.; Longhetti, L.; Mingos, D. M. P.; Briant, C. E.; Minshall, P. C.; Theobald, B. R. C.; Garlaschelli, L.; Sartorelli, U. *J. Organomet. Chem.* **1981**, *213*, 333.

(5) Cooke, C. G.; Mays, M. J. *J. Chem. Soc., Dalton Trans.* **1975**, 455. Aime, S.; Milone, L.; Osella, D.; Poli, A. *Inorg. Chim. Acta* **1978**, *30*, 45.

(6) Braunstein, P.; Rosé, J.; Granger, P.; Raya, J.; Bouaoud, S.-E.; Grandjean, D. *Organometallics* **1991**, *10*, 3686.

(7) (a) Hidai, M.; Matsuzaka, H.; Koyasu, Y.; Uchida, Y. *J. Chem. Soc., Chem. Commun.* **1986**, 1451. (b) Matsuzaka, H.; Kodama, T.; Uchida, Y.; Hidai, M. *Organometallics* **1988**, *7*, 1608.

(8) Pursiainen, J.; Ahlgren, M.; Pakkanen, T. A.; Valkonen, J. *J. Chem. Soc., Dalton Trans.* **1990**, 1147.

(9) Rossi, S.; Pursiainen, J.; Pakkanen, T. A. *J. Organomet. Chem.* **1990**, *397*, 81.

(10) Heaton, B. T. *ACS Symp. Ser.* **1983**, *No. 211*, 227.

(11) Albano, V.; Bellon, P. L.; Scatturin, V. *Chem. Commun.* **1967**, 730.

(12) Bojczuk, M.; Heaton, B. T.; Johnson, S.; Ghilardi, C. A.; Orlandini, A. *J. Organomet. Chem.* **1988**, *341*, 473.

(13) Pursiainen, J.; Pakkanen, T. A.; Jääskeläinen, J. *J. Organomet. Chem.* **1985**, *290*, 85.

(14) Pursiainen, J.; Pakkanen, T. A., unpublished results cited in ref 9.

0276-7333/92/2311-2628$03.00/0 © 1992 American Chemical Society

Downloaded via INIST-CNRS on November 13, 2020 at 16:56:55 (UTC).
See https://pubs.acs.org/sharingguidelines for options on how to legitimately share published articles.

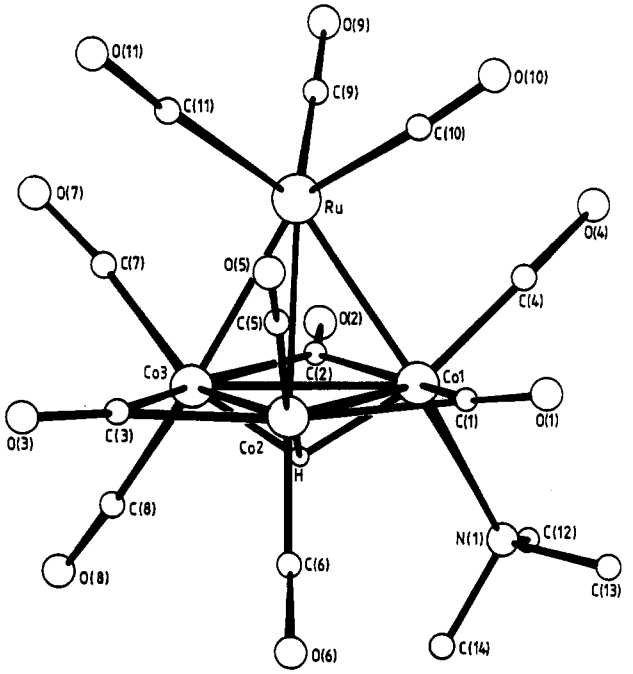
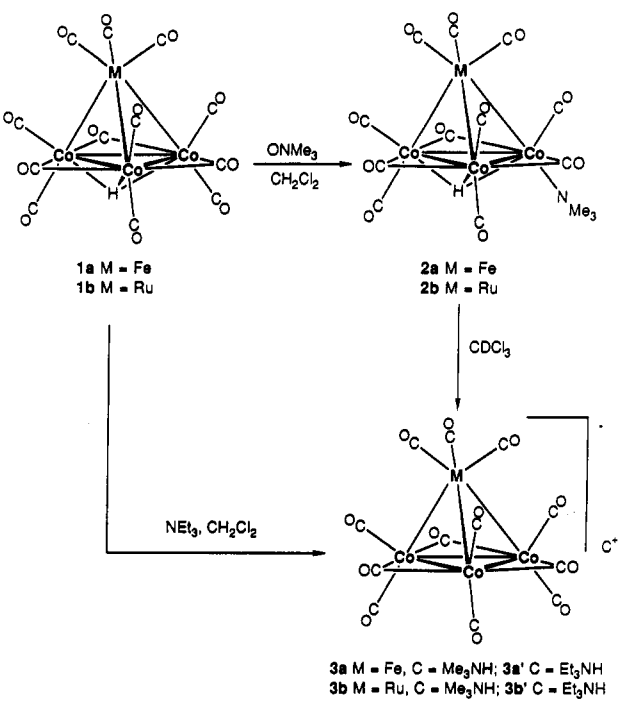


Figure 1. View of the molecular structure of **2b** with the atom labeling scheme.

Scheme I



although in $HFeCo_3(CO)_9(PMe_2Ph)_3$ the third ligand went to the apical site.[3b] The reasons for these differences are not obvious. A greater discrimination would be expected in cases where these substituents are chemically different. In $RuCo_3(CO)_{10}(PMe_2Ph)L$, the ligand L = $TeMe_2$ is bound to Ru whereas L = $TePh_2$ is bound to Co.[9]

We have recently shown[6] by ^{59}Co NMR spectroscopy that in the clusters $HMCo_3(CO)_{10}(PPh_2H)(NMe_3)$ (M = Fe, Ru), the phosphine and the amine ligands are bound to cobalt atoms. This system is particularly relevant to the studies by Hidai et al.,[7] who examined substitution of $HMCo_3(CO)_{12}$ (M = Fe, Ru) with phosphines or amines. Whereas phosphine substitution was observed at cobalt, in agreement with our findings, these authors reported that the amines NMe_3 or NEt_3 substitute a Ru-bound carbonyl. However, we could find no evidence for amine substitution at M and report here that cluster deprotonation occurs instead, yielding $[R_3NH][MCo_3(CO)_{12}]$. In addition, we describe the quantitative synthesis and crystal structure of the *cobalt*-substituted amine derivative $HRuCo_3(CO)_{11}(NMe_3)$.

Results and Discussion

Reaction of **1b** with trimethylamine *N*-oxide (1 mol equiv, CH_2Cl_2, 25 °C, 0.5 h) led to CO_2 evolution and formation of the black-red amine-substituted cluster $HRuCo_3(CO)_{11}(NMe_3)$ (**2b**) in high yield, together with a red-brown byproduct **3b** (see below) which, in contrast to **2b**, is not extractable in nonpolar solvents such as toluene. Analytical and spectroscopic data for **2b** (see Experimental Section) are consistent with its formulation as a neutral, hydrido cluster [^1H NMR (CD_2Cl_2): δ −19 ppm], of which the cobalt atom coordinated by the NMe_3 ligand [IR γ(CH) = 827 cm^{-1}] gives rise to a characteristic resonance at −1108 ppm in ^{59}Co NMR spectroscopy. Its structure was determined by X-ray diffraction (Figure 1) (see below). The Co–Co edges of the $RuCo_3$ tetrahedron are bridged by CO ligands, and the NMe_3 ligand occupies an axial position, with a Ru–Co(1)–N(1) angle of 175.9 (3)°.

When the reaction time was increased (4 h) or when acetonitrile was used as a solvent, we observed formation of **3b** at the expense of **2b**. Stirring pure **2b** in acetonitrile, acetone, or tetrahydrofuran (25 °C, 7 h) led to its complete conversion to $[Me_3NH][RuCo_3(CO)_{12}]$ (**3b**), whose ionic formulation results from analytical and spectroscopic data and comparison with $[Et_4N][RuCo_3(CO)_{12}]$[6] and with an authentic sample prepared by a double-exchange reaction between $Na[RuCo_3(CO)_{12}]$ and $[Et_3NH]Cl$ (H_2O, 25 °C, 0.25 h). In addition, **3b** readily reacts in situ with $AuCl(PPh_3)$ to give the known $RuCo_3(CO)_{12}(\mu_3\text{-}AuPPh_3)$.[16] The transformation **2b** → **3b** may be easily monitored by IR spectroscopy in the ν(CO) region. We have no indication for the formation of $[RuCo_3(CO)_{11}(NMe_3)]^-$ in the course of this process. In CH_2Cl_2, however, **2b** is stable for a few days, even upon purging the solution with CO, which one might have expected to promote the formation of **3b**. Decoordination of the amine ligand is therefore the limiting step in the progressive transformation of **2b** to **3b**, which occurs most likely via **1b** owing to partial decomposition and liberation of CO. Deprotonation of the latter has been independently shown[6] to occur in solvents sufficiently basic such as pure THF or acetone (25 °C, 3 h). It is instantaneous in the presence of 1 equiv of a base like NEt_3 (Scheme I) to give *exclusively* the red-brown, ionic complex $[Et_3NH][RuCo_3(CO)_{12}]$. Its ^1H NMR spectrum (CD_2Cl_2) contains resonances at 3.24 (q, 2 H, CH_2) and 1.42 ppm (t, 3 H, CH_3) for the ethyl groups. These values are similar but not identical with those observed by Hidai et al.[7] (solvents were not specified), which these authors assigned erroneously to $HRuCo_3(CO)_{11}(NEt_3)$. The reaction pathway is therefore similar to that observed previously[6] in the progressive transformation (CH_2Cl_2, 3 h) of $HFeCo_3(CO)_{10}(PPh_2H)(NMe_3)$ first to the stable $HFeCo_3(CO)_{11}(PPh_2H)$, which subsequently transforms ($CDCl_3$, 7 h) to $[Me_3NH][FeCo_3(CO)_{11}(PPh_2H)]$ because of the amine

(15) (a) Hure, B. T.; Knobler, C. B.; Kaesz, H. D. *J. Am. Chem. Soc.* **1978**, *100*, 3059. (b) Teller, R. G.; Wilson, R. D., McMullan, R. K.; Koetzle, T. F.; Bau, R. *J. Am. Chem. Soc.* **1978**, *100*, 3071.

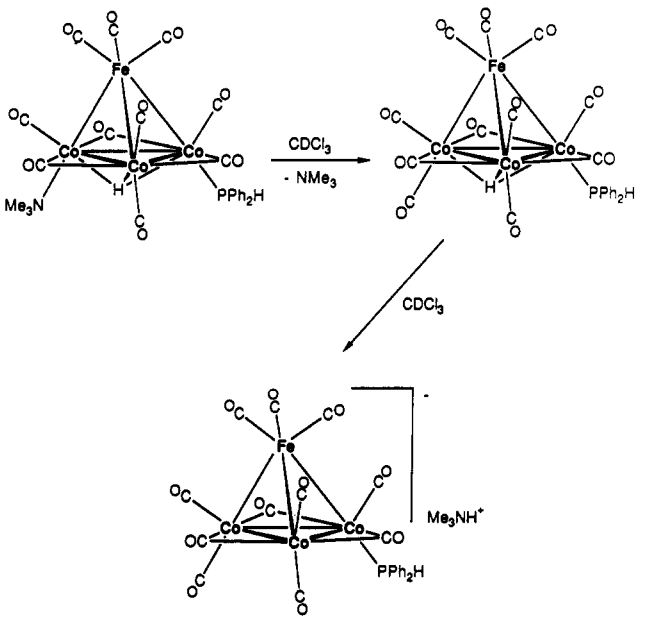
(16) (a) Braunstein, P.; Rosé, J.; Dusausoy, Y.; Mangeot, J.-P. *C.R. Acad. Sci. Paris, Ser. 2* **1982**, *294*, 967. (b) Braunstein, P.; Rosé, J.; Dedieu, A.; Dusausoy, Y.; Mangeot, J.-P.; Tiripicchio, A.; Tiripicchio Camellini, M. *J. Chem. Soc., Dalton Trans.* **1986**, 225.

Table I. Selected Infrared and ^{59}Co NMR Data

cluster	IR ν(CO), cm^{-1} (CH_2Cl_2)	NMR δ^{59}Co ($\Delta\nu_{1/2}$, Hz)[a]
$HFeCo_3(CO)_{12}$ (**1a**)	2060 vs, 2052 vs, 2030 m, 1990 m, 1887 s[b]	-2720 (420) (Co-CO)[c]
$HRuCo_3(CO)_{12}$ (**1b**)	2067 s, 2024 m, 1879 m	-2760 (1700) (Co-CO)
$HFeCo_3(CO)_{11}(NMe_3)$ (**2a**)	2080 m, 2033 vs, 2003 vs, 1967 sh, 1866 s, 1845 s	-2730 (800) (Co-CO) -910 (3200) (Co-N)
$HRuCo_3(CO)_{11}(NMe_3)$ (**2b**)	2085 w, 2049 s, 2010 s, 1860 m, 1838 m	-2747 (2000) (Co-CO) -1108 (2000) (Co-N)
$[Me_3NH][RuCo_3(CO)_{12}]$ (**3b**)	2056 m, 2024 s, 2014 s, 1972 m, 1817 m	-2617 (1800) (Co-CO)
$HRuCo_3(CO)_{11}(PPh_3)$ (**4b**)	2088 m, 2042 s, 2015 s, 1863 m, 1847 m	-2710 (4400) (Co-CO) -2564 (2800) (Co-P)
$HRuCo_3(CO)_{10}(PPh_3)_2$ (**5b**)	2065 s, 2018 m, 1996 s, 1871 sh, 1838 m, 1820 sh	-2464 (10600) (Co-CO) -2363 (3700) (Co-P)
$HRuCo_3(CO)_{11}(SEt_2)$ (**6b**)	2086 m, 2047 vs, 2036 sh, 2012 s, 1860 m, 1846 m	-2743 (2700) (Co-CO) -1970 (1390) (Co-S)
$HRuCo_3(CO)_{10}(SEt_2)_2$ (**7b**)	2068 s, 2018 s, 1995 vs, 1867 sh, 1835 m, 1820 m	-2710 (4800) (Co-CO) -1902 (2800) (Co-S)

[a] Measured at 298 K in $CDCl_3$; sample concentrations (1-2) × 10^{-2} mol/L; reference $K_3[Co(CN)_6]$ in D_2O. [b] Recorded in hexane. [c] Recorded in CD_2Cl_2.

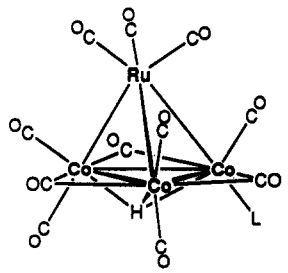
Scheme II



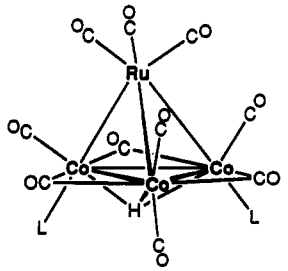
liberated (Scheme II). These transformations result in a characteristic shift of the IR ν(CO) frequencies toward lower wavenumbers (see Table I) and of the ^{59}Co NMR resonances toward higher frequencies. The single ^{59}Co resonance of **1b** in $CDCl_3$ at -2760 ppm with a half-height line width ($\Delta\nu_{1/2}$) of 1700 Hz is shifted to -2644 ppm ($\Delta\nu_{1/2}$ = 600 Hz) in acetone, reflecting the formation of the anion $[RuCo_3(CO)_{12}]^-$ [almost identical values are found for its Et_4N^+ or $(Ph_3P)_2N^+$ (PPN^+) salts]. Similarly, the single ^{59}Co NMR resonance of **3b** is found at -2617 ppm ($\Delta\nu_{1/2}$ = 1800 Hz) in $CDCl_3$. These solvent-induced chemical transformations remind us of how careful one must be in choosing and indicating the solvent in which a given spectroscopic measurement is made (its nature also significantly influences the line width at half-height of the ^{59}Co NMR resonances)!

This now explains the discrepancies between our data and those reported by Hidai et al.[7] Their value of -2648 ppm ($\Delta\nu_{1/2}$ = 740 Hz) for $HRuCo_3(CO)_{12}$ in *acetone* is in fact clearly that for [acetone H]$^+$$[RuCo_3(CO)_{12}]^-$. Similarly, the value of -2649 ppm ($\Delta\nu_{1/2}$ = 670-770 Hz) they assigned to $HRuCo_3(CO)_{11}(NMe_3)$ in *acetone* is again clearly that of an anionic species. The same holds true for their other amine-substituted hydrido clusters for which the ^{59}Co NMR spectra were all recorded in acetone. All their amine-substituted clusters were prepared in or recrystallized from THF, which has obviously led to the formation of ionic complexes and to inconsistencies in the data. It is unlikely that their "$HRuCo_3(CO)_{11}(NMe_3)$" would have survived in THF for 24 h, whereas **2b** was already completely converted to $[Me_3NH]^+[RuCo_3(CO)_{12}]^-$ after 16 h. On the basis of the above results, we think that the claim[7] for selective amine substitution at Ru in $HRuCo_3(CO)_{12}$ must be reconsidered. Rather, substitution at Co and ion-pair formation ($[R_3NH][MCo_3(CO)_{12}]$) are the only observed pathways. Reactions of Me_3NO with the isostructural $HFeCo_3(CO)_{12}$ resulted in substitution at cobalt and quantitatively yielded the amine-substituted derivative **2a**, which also transforms into the salts $[Me_3NH][FeCo_3(CO)_{12}]$ in solution. Furthermore, reactions of **1a** with NEt_3 in CH_2Cl_2 only yielded the corresponding salts $[Et_3NH][FeCo_3(CO)_{12}]$.

Cluster **2b** may be stored under N_2 at 0 °C in the solid state for weeks and represents a convenient precursor for an easy stereoselective synthesis of $HRuCo_3(CO)_{11}(L)$ clusters, monosubstituted at cobalt. The potential lability of the Co←NMe_3 bond has been evaluated through the synthesis of phosphine or thioether-substituted clusters (remember that under conditions similar to those mentioned above, CO does not displace the amine ligand of **2b** to give **1b**). Thus, room-temperature reaction of **2b** in CH_2Cl_2 with monodentate phosphine ligands instantly leads to, for example, the known $HRuCo_3(CO)_{11}(PPh_3)$ in which the phosphine is axially bound to cobalt.[7b] When SEt_2 is used as a two-electron donor ligand, it displaces NMe_3 and affords $HRuCo_3(CO)_{11}(SEt_2)$ (**6b**) in ca. 48 h.



4b L = PPh_3
6b L = SEt_2



5b L = PPh_3
7b L = SEt_2

On the basis of its spectroscopic properties, very similar to those of the structurally characterized $HRuCo_3(CO)_{11}(SMe_2)$,[17] we believe that the SEt_2 ligand is also axially bound to cobalt. The kinetics of this substitution

(17) Rossi, S.; Pursiainen, J.; Ahlgren, M.; Pakkanen, T. A. *Organometallics* **1990**, *9*, 475.

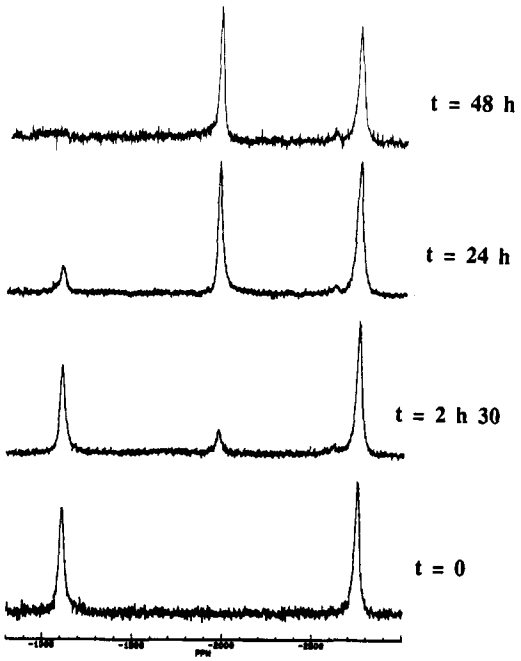


Figure 2. ^{59}Co NMR monitoring of the reaction of **2b** with SEt_2 in $CDCl_3$ showing the formation of **6b**: reaction time $t = 0$, pure **2b**; $t = 48$ h, pure **6b**.

was followed by ^{59}Co NMR (Figure 2). It thus appears that the NMe_3 ligand of **2b** may be displaced by stronger ligands. The advantage of using **2b** as a precursor becomes clear when one considers that starting from **1b** requires more forcing conditions (4–5 h under reflux) and a large excess of the SR_2 ligand.[17]

Cluster **2b** may also lead to disubstituted clusters under mild conditions. ^{59}Co NMR monitoring of its reaction with Me_3NO in $CDCl_3$ showed the formation of the new, labile $HRuCo_3(CO)_{10}(NMe_3)_2$ in which two cobalt atoms carry each an amine ligand (see Experimental Section) (Figure 3). It rapidly transforms into $[RuCo_3(CO)_{12}]^-$, owing to partial fragmentation and liberation of CO. This contrasts with the slower evolution of $HRuCo_3(CO)_{10}(NMe_3)(PPh_2H)$ first into $HRuCo_3(CO)_{11}(PPh_2H)$, which is subsequently deprotonated by the free amine present to give $[RuCo_3(CO)_{11}(PPh_2H)]^-$ and $[RuCo_3(CO)_{12}]^-$. We could also detect $HFeCo_3(CO)_{10}(NMe_3)_2$ (see Experimental Section) (Figure 4), which is a very labile species.

Cluster **2b** reacts with excess PPh_3 or SEt_2 (the presence of 1 equiv of Me_3NO allows the use of only 2 equiv of ligand) to give the disubstituted derivatives **5b** and **7b**, respectively. Their spectroscopic data (Table I) show clearly that the second ligand is bound to another Co atom, consistent with the solid-state structure of **5b**[13] and data obtained independently by Pakkanen et al. for $HRuCo_3(CO)_{10}(SMe_2)_2$.[17] It is interesting that the reaction of **2b** with Me_3NO does not lead to CO substitution at Ru, in contrast to the reactions of $HRuCo_3(CO)_{11}(PMe_2Ph)$ with $TeMe_2$ or PMe_2Ph.[9,14]

Crystal Structure of $RuCo_3(\mu_3\text{-}H)(\mu\text{-}CO)_3(CO)_8(NMe_3)$ (2b). The molecular structure of **2b** has been determined by X-ray diffraction and is shown in Figure 1. Bond lengths and relevant bond angles are given in Tables II and III, respectively. The Ru–Co and Co–Co distances in this tetrahedral cluster are in the range found for these bonds in the related molecules $[PPN][RuCo_3(CO)_{12}]$,[18] $RuCo_3(\mu_3\text{-}H)(CO)_{11}(L)$ (L = PPh_3,[7b] PMe_3, or

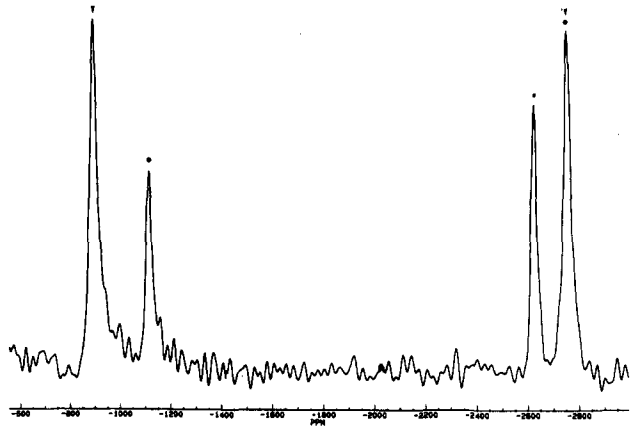


Figure 3. ^{59}Co NMR spectrum of the reaction mixture of **2b** with Me_3NO: (●) **2b**, (▼) $HRuCo_3(CO)_{10}(NMe_3)_2$, (*) $[RuCo_3(CO)_{12}]^-$ (−2617 ppm).

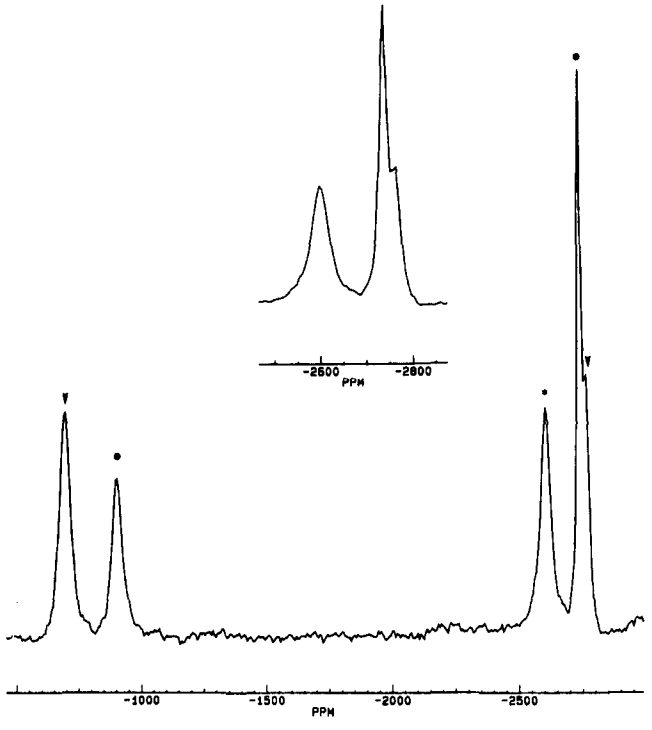


Figure 4. ^{59}Co NMR spectrum of the reaction mixture of **2a** with Me_3NO: (●) **2a**, (▼) $HFeCo_3(CO)_{10}(NMe_3)_2$, (*) $[FeCo_3(CO)_{12}]^-$ (−2597 ppm).

PMe_2Ph,[8] $TePh_2$,[9] SMe_2,[17] $SeMe_2$[19]), and $RuCo_3(\mu_3\text{-}AuPPh_3)(CO)_{12}$.[16] A carbonyl ligand bridges each Co–Co bond, and C(1)–O(1) and C(2)–O(2) are slightly closer to the amine-substituted Co atom. The axial disposition of the NMe_3 ligand is as anticipated and is comparable to the situation in $RuCo_3(\mu_3\text{-}H)(CO)_{11}(PPh_3)$,[7b] although equatorial phosphines have been encountered in tetrahedral clusters.[8] The Ru(1)–Co(1)–C(4) angle of 85.1 (3)° is significantly larger than the other Ru–Co–$C_{equatorial}$ angles. A similar effect is observed in the structure of $FeCo_3(\mu_3\text{-}H)(CO)_{11}(PPh_2H)$[6] and $RuCo_3(\mu_3\text{-}H)(CO)_{11}(PPh_3)$.[7b] The difference between the Co–N distance in **2b** [2.103 (9) Å] and the Co–P distance in $RuCo_3(\mu_3\text{-}H)(CO)_{11}(PPh_3)$ [2.261 (5) Å][7b] is smaller than the difference between the atomic radii of N and P (0.4 Å). This could be related to a greater lability of the amine ligand. Similar observations were made in $Os_3(CO)_9(NO)_2(NMe_3)$.[20] The hydride lig-

(18) Hidai, M.; Orisaku, M.; Ue, M.; Koyasu, Y.; Kodama, T.; Uchida, Y. *Organometallics* **1983**, *2*, 292.

(19) Rossi, S.; Pursiainen, J.; Ahlgren, M.; Pakkanen, T. A. *J. Organomet. Chem.* **1990**, *391*, 403.

Table II. Bond Distances (Å) of 2b[a]

Ru-Co(1)	2.626 (1)	Co(1)-H	1.69 (9)	O(3)-C(3)	1.167 (12)
Ru-Co(2)	2.628 (1)	Co(2)-C(1)	1.994 (10)	O(4)-C(4)	1.142 (12)
Ru-Co(3)	2.627 (1)	Co(2)-C(3)	1.953 (9)	O(5)-C(5)	1.138 (12)
Co(1)-Co(2)	2.511 (2)	Co(2)-C(5)	1.759 (10)	O(6)-C(6)	1.138 (13)
Co(1)-Co(3)	2.510 (2)	Co(2)-C(6)	1.807 (11)	O(7)-C(7)	1.161 (13)
Co(2)-Co(3)	2.494 (2)	Co(2)-H	1.70 (9)	O(8)-C(8)	1.130 (12)
Ru-C(9)	1.884 (11)	Co(3)-C(2)	1.984 (9)	O(9)-C(9)	1.128 (13)
Ru-C(10)	1.891 (12)	Co(3)-C(3)	1.984 (10)	O(10)-C(10)	1.133 (13)
Ru-C(11)	1.914 (11)	Co(3)-C(7)	1.722 (11)	O(11)-C(11)	1.121 (12)
Co(1)-N(1)	2.103 (9)	Co(3)-C(8)	1.795 (11)	N(1)-C(12)	1.32 (3)
Co(1)-C(1)	1.902 (10)	Co(3)-H	1.55 (8)	N(1)-C(13)	1.39 (3)
Co(1)-C(2)	1.941 (10)	O(1)-C(1)	1.173 (11)	N(1)-C(14)	1.37 (2)
Co(1)-C(4)	1.737 (11)	O(2)-C(2)	1.126 (11)		

[a] Numbers in parentheses are estimated standard deviations in the least significant digits.

Table III. Selected Bond Angles (deg) of 2b[a]

Co(2)-Co(1)-Ru	61.49 (4)	Co(1)-Co(2)-C(5)	126.1 (4)
Co(3)-Co(1)-Ru	61.46 (4)	Co(1)-Co(2)-C(6)	119.3 (3)
Co(1)-Co(2)-Ru	61.42 (5)	Co(1)-Co(2)-H	42 (3)
Co(3)-Co(2)-Ru	61.63 (4)	Co(3)-Co(2)-C(1)	108.3 (3)
Co(1)-Co(3)-Ru	61.45 (4)	Co(3)-Co(2)-C(3)	51.3 (3)
Co(2)-Co(3)-Ru	61.69 (4)	Co(3)-Co(2)-C(5)	126.1 (4)
Co(1)-Ru-Co(2)	57.09 (4)	Co(3)-Co(2)-C(6)	122.1 (3)
Co(1)-Ru-Co(3)	57.09 (4)	Co(3)-Co(2)-H	38 (3)
Co(2)-Ru-Co(3)	56.68 (4)	Co(2)-Co(1)-N(1)	114.9 (3)
Co(1)-Co(3)-Co(2)	60.23 (5)	Co(2)-Co(1)-C(1)	51.5 (3)
Co(1)-Co(2)-Co(3)	60.20 (5)	Co(2)-Co(1)-C(2)	110.5 (3)
Co(2)-Co(1)-Co(3)	59.58 (4)	Co(2)-Co(1)-C(4)	133.7 (3)
Ru-Co(1)-N(1)	175.9 (3)	Co(2)-Co(1)-H	42 (3)
Ru-Co(1)-C(1)	81.8 (4)	Co(2)-Co(3)-C(2)	109.6 (3)
Ru-Co(1)-C(2)	82.4 (3)	Co(2)-Co(3)-C(3)	50.1 (3)
Ru-Co(1)-C(4)	85.1 (3)	Co(2)-Co(3)-C(7)	125.2 (4)
Ru-Co(1)-H	84 (3)	Co(2)-Co(3)-C(8)	122.4 (3)
Ru-Co(2)-C(1)	80.2 (3)	Co(2)-Co(3)-H	42 (3)
Ru-Co(2)-C(3)	84.5 (3)	Co(3)-Co(1)-N(1)	115.3 (3)
Ru-Co(2)-C(5)	76.4 (4)	Co(3)-Co(1)-C(1)	110.9 (3)
Ru-Co(2)-C(6)	176.2 (3)	Co(3)-Co(1)-C(2)	51.0 (3)
Ru-Co(2)-H	84 (3)	Co(3)-Co(1)-C(4)	132.2 (3)
Ru-Co(3)-C(2)	81.6 (3)	Co(3)-Co(1)-H	37 (3)
Ru-Co(3)-C(3)	84.0 (1)	Co(1)-C(4)-O(4)	177.7 (9)
Ru-Co(3)-C(7)	75.6 (4)	Co(1)-C(2)-O(2)	142.2 (8)
Ru-Co(3)-C(8)	175.5 (3)	Co(3)-C(2)-O(2)	137.9 (8)
Ru-Co(3)-H	87 (3)	Co(1)-C(1)-O(1)	145.5 (8)
Co(1)-Ru-C(9)	99.1 (3)	Co(2)-C(1)-O(1)	134.1 (8)
Co(1)-Ru-C(10)	99.8 (4)	Co(2)-C(5)-O(5)	172 (1)
Co(1)-Ru-C(11)	160.0 (3)	Co(2)-C(6)-O(6)	177 (1)
Co(2)-Ru-C(9)	153.7 (3)	Co(2)-C(3)-O(3)	140.6 (8)
Co(2)-Ru-C(10)	101.8 (4)	Co(3)-C(3)-O(3)	140.8 (8)
Co(2)-Ru-C(11)	106.4 (4)	Co(3)-C(7)-O(7)	170 (1)
Co(3)-Ru-C(9)	102.4 (3)	Co(3)-C(8)-O(8)	175 (1)
Co(3)-Ru-C(10)	153.8 (4)	Co(1)-N(1)-C(12)	116 (1)
Co(3)-Ru-C(11)	105.4 (3)	Co(1)-N(1)-C(13)	114 (1)
Co(1)-Co(2)-C(1)	48.3 (3)	Co(1)-N(1)-C(14)	115.2 (9)
Co(1)-Co(2)-C(3)	111.4 (3)		

[a] Numbers in parentheses are estimated standard deviations in the least significant digits.

and was located in the Fourier difference map and refined at 0.7 (1) Å below the $Co_3C(1)$-C(2)-C(3) mean plane, in excellent agreement with the analogous distance of ca. 0.75 Å observed in $FeCo_3(\mu_3\text{-}H)(CO)_9[P(OMe)_3]_3$[15] or 0.76 [0.87] Å in $FeCo_3(\mu_3\text{-}H)(CO)_{11}(PPh_2H)$ (two independent molecules).[6]

Conclusion

In view of the large number of homo- and heteronuclear cobalt-containing clusters of structural or catalytic interest,[21] ^{59}Co NMR spectroscopy should continue to prove a very useful method to improve our knowlege about metallosite selectivity in cluster reactions. We have recently shown that ^{99}Ru studies can also be extended to cluster complexes such as $HRuCo_3(CO)_{12}$.[22] From our investigations of the regiochemistry in monosubstitution reactions of $HMCo_3(CO)_{12}$ (M = Fe, Ru) with phosphines or amines, we conclude that these ligands will substitute a Co-bound carbonyl. We also observe that amines readily deprotonate such hydrido clusters but do not tend to substitute Ru-bound carbonyl ligands, in contrast to a previous report.[7] In the disubstituted clusters $HMCo_3(CO)_{10}L_2$ (L = NMe_3, PPh_3, SEt_2), ^{59}Co NMR spectroscopy clearly showed that both L ligands are coordinated to cobalt atoms. We are currently investigating the combined use of IR and ^{59}Co NMR spectroscopic methods for the solution study of new systems where regioisomers could form. These results should then be correlated with the molecular structures in the solid state.

Experimental Section

General Procedures. Standard Schlenk line techniques were used, and manipulations were carried out under a purified nitrogen atmosphere. Solvents were distilled before use. $HFeCo_3(CO)_{12}$[23] and $HRuCo_3(CO)_{12}$[6] were prepared by use of published procedures. SEt_2, $Me_3NO{\cdot}2H_2O$, and all organophosphines were commercial samples and were used as received. Solution infrared spectra were recorded on a Perkin-Elmer 398 in 0.1-mm matched BaF_2 cells. The UV-visible spectra were recorded on a Schimadzu UV-260. NMR spectra were measured on a Bruker MSL-300 instument (^{59}Co, 71.21 MHz). The chemical shifts reported (ppm) for ^{59}Co are positive high frequency from the external reference $K_3[Co(CN)_6]$ saturated in D_2O. Standard parameters are as follows: pulse width 3 μs, sweep width 263 kHz, number of scans between 5000 and 100000. Spectroscopic data for the complexes are given in Table I. When product stability allowed, elemental analyses are given.

Preparation of $HRuCo_3(CO)_{11}(NMe_3)$ (2b). To a solution of $HRuCo_3(CO)_{12}$ (0.368 g, 0.598 mmol) in CH_2Cl_2 (30 mL) was added solid $Me_3NO{\cdot}2H_2O$ (0.068 g, 0.612 mmol). The deep red reaction mixture became immediately red-brown. After being stirred for 0.25 h at room temperature, the solution was filtered and the solvent was evaporated in vacuo. The resulting solid was washed with hexane [elimination of unreacted $HRuCo_3(CO)_{12}$] and then extracted with toluene (80 mL). The toluene solution was evaporated to dryness, giving the title product as black microcrystals (0.310 g, 80%). MS: m/e 646 (M^+). UV (CH_2Cl_2): λ_{max} 305, 386, 503, 590 (sh) nm. ^1H NMR (CD_2Cl_2): δ 2.21 (s, NMe_3), −19 (large, H). Anal. Calcd for $C_{14}H_{10}Co_3NO_{11}Ru$: C, 26.03; H, 1.56; N, 2.17. Found: C, 26.3; H, 1.6; N, 2.2.

Preparation of $HFeCo_3(CO)_{11}(NMe_3)$ (2a). This cluster was prepared by the same procedure as for **2b**. Evaporation of the toluene solution gave **2a** as a black powder in 52% yield. UV (CH_2Cl_2): λ_{max} 306, 330 (sh), 390 (sh), 572, 670 (sh) nm. Anal.

(20) Johnson, B. F. G.; Lewis, J.; Raithby, P. R.; Zuccaro, C. *J. Chem. Soc., Chem. Commun.* **1979**, 916.

(21) Braunstein, P.; Rosé, J. Heterometallic Clusters in Catalysis. In *Stereochemistry of Organometallic and Inorganic Compounds*, Bernal, I., Ed.; Elsevier: Amsterdam, 1989; Vol. 3, pp 3–138.

(22) Braunstein, P.; Rosé, J.; Granger, P.; Richert, T. *Magn. Reson. Chem.* **1991**, *29*, S31.

(23) Chini, P.; Colli, L.; Peraldo, M. *Gazz. Chim. Ital.* **1960**, *90*, 1005.

Table IV. Crystal Data and Data Collection for 2b

formula	$C_{14}H_{10}Co_3NO_{11}Ru$
fw	646.1
cryst system	orthorombic
space group	$Pna2_1$
cryst dimens, mm	0.24 × 0.20 × 0.16
cryst color	black
a, Å	16.877 (5)
b, Å	10.296 (2)
c, Å	11.946 (2)
α, deg	90
β, deg	90
γ, deg	90
V, Å^3	2705.8
Z	4
ρ_{calcd}, g/cm^3	2.067
F(000)	1256
temp, °C	25
diffractometer	Enraf-Nonius CAD-4
radiation (graphite monochromator)	Mo Kα (λ = 0.71073 Å)
linear abs coeff, cm^{-1}	31.086
scan type	$\omega/2\theta$
scan width, deg	(1 + 0.35 tan θ)
θ limits, deg	1–24
systematic absences	$0kl$ $k + 1 \neq 2n$; $h0l$ $h \neq 2n$; $00l$ $l \neq 2n$
octants collected	$+h,+k,+l$
no. of data collected	2113
no. of unique data used	1471 [$F_o^2 > 3\sigma(F_o^2)$]
no. of variables	275
$R = \sum(\|\|F_o\| - \|F_c\|\|)/\sum\|F_o\|$	0.026
R_w[a]	0.035
GOF[b]	1.050
largest shift/esd, final cycle	0.01
largest peak in final diff map, e/Å^3	0.469
fudge factor	0.05

[a] $R_w = [\sum w(|F_o| - |F_c|)^2/\sum w|F_o|^2]^{1/2}$. [b] GOF = $[\sum w(|F_o| - |F_c|)^2/N$ observ − N params$]^{1/2}$.

Calcd for $C_{14}H_{10}Co_3FeNO_{11}$: C, 27.99; H, 1.68; N, 2.33. Found: C, 28.4; H, 1.7; N, 2.5.

Tranformation of 2b in Organic Solvents. When cluster **2b** was stirred in CH_2Cl_2 at room temperature, the red-brown solution progressively became orange red and a precipitate was formed. IR monitoring of the reaction indicated the progressive disappearance of the ν(CO) bands corresponding to **2b** and the formation of new bands attributed to the anionic species $(Me_3NH)[RuCo_3(CO)_{12}]$ (**3b**). After 1 week a complete transformation was achieved. When a more polar solvent such as THF was used, the transformation was completed after a few hours. ^{59}Co NMR monitoring was also used to study this transformation.

Reaction of 2b with PPh_3. To a solution of **2b** (0.100 g, 0.155 mmol) in CH_2Cl_2 (20 mL) was added solid PPh_3 (0.041 g, 0.156 mmol). The violet-red mixture became slowly deep red. The reaction mixture was stirred at room temperature until **2b** had disappeared (2 days). This reaction was best monitored by thin-layer chromatography. The solution was filtered, and the solvent was evaporated in vacuo. The resulting solid was extracted with hexane, and pure $HRuCo_3(CO)_{11}(PPh_3)$ (**4b**) was obtained as black-red microcrystals by cooling this solution to −15 °C (0.070 g, 53%). UV (CH_2Cl_2): λ_{max} 317, 384, 492, 570 (sh) nm. Anal. Calcd for $C_{29}H_{16}Co_3O_{11}PRu$: C, 41.01; H, 1.90. Found: C, 40.8; H, 1.8.

Preparation of $HRuCo_3(CO)_{10}(PPh_3)_2$ (5b). To a suspension of **2b** (0.050 g, 0.078 mmol) in $MeNO_2$ (10 mL) was added solid PPh_3 (0.041 g, 0.156 mmol). After 0.5-h stirring at room temperature, black needles of $HRuCo_3(CO)_{10}(PPh_3)_2$ were formed and separated by filtration (0.032 g, 38%). UV (CH_2Cl_2): λ_{max} 317, 385, 520, 600 (sh) nm. Anal. Calcd for $C_{46}H_{31}Co_3O_{10}P_2Ru$: C, 50.99; H, 2.88. Found: C, 51.2; H, 3.0.

Reaction of 2b with SEt_2. To a solution of **2b** (0.100 g, 0.155 mmol) in CH_2Cl_2 (20 mL) was added an excess of SEt_2 (0.034 mL, 0.314 mmol), and the reaction mixture was stirred for 1 day at room temperature. The resulting solution was filtered and chromatographed over silica gel. Using a hexane/toluene mixture (3:1) as eluent gave a reddish brown and a violet band. $HRuCo_3(CO)_{11}(SEt_2)$ (**6b**) was recovered from the first band, dried in vacuo, and recrystallized from hexane at −15 °C (0.055 g, 52%). UV (CH_2Cl_2): λ_{max} 319, 387, 500, 580 (sh) nm. Anal. Calcd for $C_{15}H_{11}Co_3O_{11}RuS$: C, 26.61; H, 1.64. Found: C, 26.4; H, 1.8. The violet band afforded the disubstituted cluster $HRuCo_3(CO)_{10}(SEt_2)_2$ (**7b**) (0.020 g, 17%). UV (CH_2Cl_2): λ_{max} 310, 400, 555, 630 (sh) nm. Anal. Calcd for $C_{18}H_{21}Co_3O_{10}RuS_2$: C, 29.24; H, 2.86. Found: C, 29.0; H, 2.7.

Table V. Positional Parameters and Their Estimated Standard Deviations[a]

atom	x	y	z	B, Å^2
Ru	0.92528 (4)	0.15153 (6)	0.383	3.09 (1)
Co(1)	0.86865 (6)	0.3835 (1)	0.4272 (1)	2.76 (2)
Co(2)	0.90591 (6)	0.2388 (1)	0.5879 (1)	2.79 (2)
Co(3)	1.01164 (6)	0.3383 (1)	0.4699 (1)	2.84 (2)
O(1)	0.7356 (4)	0.2532 (8)	0.5403 (6)	5.4 (2)
O(2)	0.9820 (4)	0.4888 (8)	0.2671 (6)	5.1 (2)
O(3)	1.0683 (4)	0.1639 (8)	0.6523 (7)	6.0 (2)
O(4)	0.7772 (4)	0.3479 (8)	0.2261 (6)	5.7 (2)
O(5)	0.8705 (5)	−0.0331 (7)	0.6206 (7)	6.4 (2)
O(6)	0.8724 (5)	0.3209 (8)	0.8193 (5)	5.7 (2)
O(7)	1.1271 (4)	0.212 (1)	0.3308 (7)	7.7 (2)
O(8)	1.1218 (5)	0.5377 (8)	0.5480 (8)	7.0 (2)
O(9)	0.9567 (6)	0.1830 (9)	0.1363 (6)	7.2 (2)
O(10)	0.7730 (5)	0.005 (1)	0.3401 (8)	8.1 (2)
O(11)	1.0277 (5)	−0.0902 (8)	0.3955 (7)	7.8 (2)
N(1)	0.8282 (5)	0.5692 (7)	0.4733 (8)	4.7 (2)
C(1)	0.8010 (5)	0.286 (1)	0.5226 (7)	3.7 (2)
C(2)	0.9626 (5)	0.4384 (9)	0.3461 (7)	3.2 (2)
C(3)	1.0207 (5)	0.2183 (9)	0.5993 (8)	3.5 (2)
C(4)	0.8122 (5)	0.3615 (9)	0.3071 (8)	3.8 (2)
C(5)	0.8850 (6)	0.0720 (9)	0.5995 (8)	4.2 (2)
C(6)	0.8867 (5)	0.2923 (9)	0.7294 (8)	3.6 (2)
C(7)	1.0765 (5)	0.254 (1)	0.3857 (9)	4.5 (2)
C(8)	1.0767 (5)	0.463 (1)	0.5215 (8)	4.1 (2)
C(9)	0.9439 (6)	0.172 (1)	0.2285 (8)	3.9 (2)
C(10)	0.8294 (6)	0.061 (1)	0.359 (1)	5.4 (3)
C(11)	0.9887 (6)	−0.002 (1)	0.3948 (9)	4.6 (2)
C(12)	0.838 (2)	0.661 (1)	0.397 (2)	22.2 (9)
C(13)	0.748 (1)	0.574 (1)	0.498 (3)	15.7 (7)
C(14)	0.860 (1)	0.618 (1)	0.570 (2)	19.7 (5)
H	0.936 (4)	0.382 (8)	0.532 (7)	3 (2)*
H(12A)	0.8175	0.7409	0.4255	5*
H(12B)	0.8921	0.6703	0.3803	5*
H(12C)	0.8093	0.6382	0.3312	5*
H(13A)	0.7335	0.6604	0.5176	5*
H(13B)	0.7181	0.5483	0.4336	5*
H(13C)	0.7363	0.5173	0.5581	5*
H(14A)	0.8388	0.7018	0.5840	5*
H(14B)	0.8483	0.5620	0.6305	5*
H(14C)	0.9161	0.6248	0.5616	5*

[a] Starred atoms were refined isotropically. Anisotropically refined atoms are given in the form of the isotropic equivalent displacement parameter: $(^4/_3)[a^2\beta(1,1) + b^2\beta(2,2) + c^2\beta(3,3) + ab(\cos\gamma)\beta(1,2) + ac(\cos\beta)\beta(1,3) + bc(\cos\alpha)\beta(2,3)]$.

Reactions of 2 with Me_3NO. This reaction was performed in a NMR tube for direct monitoring. To a sample of **2b** (0.020 g) dissolved in $CDCl_3$ (2 mL) in a NMR tube was added an excess of solid Me_3NO. The progress of the reaction was monitored by ^{59}Co NMR spectroscopy, showing (Figure 2) the rapid development of new resonances at −890 ppm, which corresponds to a new amine-substituted Co in $HRuCo_3(CO)_{10}(NMe_3)_2$, and at −2617 ppm, which is that of $[RuCo_3(CO)_{12}]^-$. The resonance of the unsubstituted Co nucleus in $HRuCo_3(CO)_{10}(NMe_3)_2$ overlaps with that of **2b**. The spectral evolution with time indicates the disappearance of the resonance at −890 ppm after few minutes.

Similarly, the reaction of **2a** with Me_3NO yielded the labile $HFeCo_3(CO)_{10}(NMe_3)_2$, which has ^{59}Co resonances at −695 (amine-substituted Co atom) and −2757 ppm (unsubstituted Co atom) (Figure 4). The latter resonance is now resolved from that of **2a**, which has a much smaller $\Delta\nu_{1/2}$ value than **2b** (see Table I).

Crystallographic Data, Structure Solution, and Refinement of 2b. Suitable black crystals of **2b** were obtained by slow crystallization of the compound from a hexane solution at −15 °C. Diffraction measurements were carried out at room temperature on a Nonius CAD-4 four-circle diffractometer using graphite-monochromatized Mo Kα radiation. Unit cell parameters were calculated from the setting angles of 25 carefully centered

reflections. Crystal data and intensity collections parameters are given in Table IV. The intensities of three reflections (006, 5$\bar{2}$2, 4$\bar{2}$0) were monitored every hour of exposure and showed no evidence of decay. For all subsequent computations the Enraf-Nonius SDP package was used.[24] Data were corrected for Lorentz polarization and for absorption using the DIFABS program[25] (absorption coefficients minimum 0.951, maximum 1.024). The crystal structure was solved by using the Patterson and Fourier difference methods and refined by full-matrix least squares with anisotropic thermal parameters for all non-hydrogen atoms. The function minimized was $\sum(w|F_o| - |F_c|)^2$, where the weight w is $[4F_o^2]/[\sigma^2(F_o) - (0.07|F_o|^2)]$. Hydrogen atoms were placed in calculated positions (C-H distances 0.95 Å) in structure factor calculations and were assigned isotropic thermal parameters of $B = 5$ Å^2, except for the hydrido H, which was positioned by Fourier difference and refined isotropically. A final difference map revealed no significant residual peak. Neutral atom scattering factors used for all atoms and anomalous dispersion coefficients were obtained from standard sources.[26] The positional parameters obtained from the last cycle of refinement are listed in Table V, with the corresponding standard deviations.

Acknowledgment. We thank the "Region Alsace" for its participation in the purchase of the MSL 300 instrument and the "Commission of the European Communities" for financial support (Contract ST2J-0479-C).

Supplementary Material Available: Projection of the structure of **2b** perpendicular to the Co_3 plane (Figure S-1), complete set of bond angles (Table S-I), and temperature factors for anisotropic atoms (Table S-II) (4 pages). Ordering information is given on any current masthead page.

OM920053S

(24) Frenz, B. A. In *Computing in Crystallography*; Schenk, H., Olthof-Hazekamp, R., van Koningsveld, H., Bassi, G. C., Eds.; Delft University Press: Delft, The Netherlands, 1978; pp 64-71.
(25) Walker, N.; Stuart, D. *Acta Crystallogr.* **1983**, *A39*, 158.
(26) *International Tables for X-Ray Crystallography*; Kynoch: Birmingham, 1974; Vol. IV, p 99.

Control of Donor-Acceptor Interactions in Organoalkaline-Earth-Transition-Metal Complexes. Crystallographic Characterization of $(Me_5C_5)_2HfCl(\mu\text{-}Cl)Ca(Me_5C_5)_2$

S. Craig Sockwell, Pamela S. Tanner, and Timothy P. Hanusa*

Department of Chemistry, Vanderbilt University, Nashville, Tennessee 37235

Received September 6, 1991

The problem of ligand exchange or loss in the formation of organometallic alkaline-earth-transition-metal complexes can be minimized by ensuring that any exchange would be degenerate or would require an unfavorable transfer of ligands. This approach is illustrated in the formation of chloride-bridged calcium-group 4 dimers and in an isocarbonyl-linked calcium-chromium dimer. Bis(pentamethylcyclopentadienyl)calcium Cp^*_2Ca, reacts with $Cp^*_2ZrCl_2$, $Cp^*_2HfCl_2$, and $Cp^*_2ThCl_2$ in toluene to yield 1:1 adducts. Orange-yellow crystals of $Cp^*_2HfCl(\mu\text{-}Cl)CaCp^*_2$ grown from toluene are triclinic, space group $P\bar{1}$, with $a = 11.146$ (4) Å, $b = 16.942$ (6) Å, $c = 11.109$ (3) Å, $\alpha = 103.34$ (3)°, $\beta = 94.89$ (3)°, $\gamma = 102.50$ (3)°, and D(calcd) = 1.398 g cm^{-3} for $Z = 2$. The structure consists of two bent metallocene units with a single μ-Cl and a terminal Cl on hafnium: Ca-μ-Cl = 2.864 (3) Å, Hf-μ-Cl = 2.463 (3) Å, Hf-Cl(t) = 2.383 (3) Å, and Ca-Cl-Hf = 161.3 (1)°. Cp^*_2Ca reacts with $Cp^*_2Zr(CO)_2$ and mesitylenechromium tricarbonyl in toluene in yield 1:1 adducts. In the solid state, the calcium-chromium adduct exists as a tetranuclear species, constructed around a 12-membered ring consisting of two Ca and Cr atoms and four carbonyl groups.

The heavy alkaline-earth (Ae) elements calcium, strontium, and barium are being increasingly incorporated into a range of solid-state materials with diverse electronic and chemical properties, including the high-temperature superconductors (e.g., $YBa_2Cu_3O_{7-x}$),[1-3] "hydrogen storage" alloys (e.g., $CaNi_5$),[4] and perovskite-based methane oxidation catalysts (e.g., ABO_3 (A = Ca, Sr, Ba; B = Ti, Zr, Ce)).[5,6] Rational syntheses of discrete polymetallic group 2-transition-metal complexes that might serve either as precursors to or as models of these nonmolecular solids have been limited to O-bound (primarily alkoxide) species,[7] and facile ligand exchange or loss can make controlling the composition of these systems difficult.[8]

Table I. ^{1}H NMR Shifts of Heterometallic Compounds

compd	heterometallic subunits $(C_5Me_5)Ca$	heterometallic subunits $(C_5Me_5)M$	parent $(C_5Me_5)ME_2$	ref
$Cp^*_2Ca(Cl)_2ZrCp^*_2$	2.04	1.80	1.84	17
$Cp^*_2Ca(Cl)_2HfCp^*_2$	1.95	1.89	1.90	15
$Cp^*_2Ca(Cl)_2ThCp^*_2$	2.14	2.09	2.02	18
$Cp^*_2Ca(OC)_2ZrCp^*_2$	2.07	1.70	1.73	16
$Cp^*_2Ca(\mu\text{-}OC)_2(OC)\text{-}Cr(mes)$	2.15	(4.13, 1.64)[a]	(4.07, 1.66)[a]	22

[a] The values for the ring and methyl protons, respectively, of the mesitylene group.

(1) Berry, A. D.; Gaskill, R. T.; Holm, E. J.; Cukauskas, R.; Kaplan, R.; Henry, R. L. *Appl. Phys. Lett.* **1988**, *52*, 1743-1745.
(2) Panson, A. J.; Charles, R. G.; Schmidt, D. N.; Szedon, J. R.; Machiko, G. J.; Braginski, A. I. *Appl. Phys. Lett.* **1988**, *53*, 1756-1758.
(3) Richeson, D. S.; Tonge, L. M.; Zhao, J.; Zhang, J.; Marcy, H. O.; Marks, T. J.; Wessels, B. W.; Kannewurf, C. R. *Appl. Phys. Lett.* **1989**, *54*, 2154-2156.
(4) Willems, J. J. G.; Buschow, K. H. J. *J. Less-Comm. Met.* **1987**, *129*, 13-30.
(5) Nagamoto, H.; Amanuma, K.; Nobutomo, H.; Inoue, H. *Chem. Lett.* **1988**, *2*, 237-240.
(6) Pereira, P.; Lee, S. H.; Somorjai, G. A.; Heinemann, H. *Catal. Lett.* **1990**, *6*, 255-262.
(7) Caulton, K. G.; Hubert, P. L. G. *Chem. Rev.* **1990**, *90*, 969-995.

0276-7333/92/2311-2634$03.00/0 © 1992 American Chemical Society